Increase in Capacitance by Subnanometer Pores in Carbon

Electrical double-layer capacitors (EDLCs, also known as supercapacitors or ultracapacitors) store energy by electrosorption of ions at the electrode/electrolyte interface.[1] To achieve a high-energy storage capacity, electrodes with a high surface area and well-developed pore structure in the range from several Angstroms to several tens of nanometers are required.[2] However, neither natural precursor-derived carbons nor templated carbon materials present an ideal, infinitesimally narrow pore size dispersion.[3]

In EDLCs, the use of salt dissolved in an organic or aqueous solvent makes it important to consider the solvation shell around the ions. The bare ion size is usually below 1 nm, whereas the solvation shell can increase the size significantly.[3] Several studies have provided strong evidence of ion desolvation during electrosorption, which is the only way to explain why carbon materials with pore sizes smaller than the solvated ion but larger than the bare ion have high charge storage capacities.[4−8] A maximized capacitance (normalized by the surface area) was found in experimental and theoretical studies when matching the pore size with the ion size.[9] This effect seems to be universally applicable for solvent-containing and solvent-free electrolytes (ionic liquids), while important secondary differences are to be considered for the latter. For example, the oscillatory dependency of capacitance on pore size predicted for neat ionic liquids and ideal carbons with slit pores is lost when introducing a solvent, where a single maximum is observed when the ion size and the pore size are identical.[10,11]

This Viewpoint clarifies the correlation between capacitance and pore size, which is of high practical importance for the design of advanced carbon electrode materials. Two extreme cases are obvious: excessively large pores, accompanied by large pore volumes and limited specific surface area, will lead to a low energy storage capacity, whereas very small pores will limit the ion access due to steric effects (Figure 1), in addition to imposing obstacles to ion transport.[12,13] Yet, for the intermediate range, down to the point when the pores are too small for the bare ion to fit, there is no consent in the literature about the correlation between the pore size and the corresponding area-normalized capacitance. For example, there has been criticism about the method of surface area determination and normalization, especially considering the inadequacy of the Brunauer−Emmett−Teller (BET) model for microporous carbons.[14,15] Benchmarking various kinds of carbons, including carbon monoliths, a "regular pattern" was presented, suggesting that the area-normalized capacitance does not depend on the pore size.[14,16] This lack of dependence can be explained by neither the ab initio or molecular dynamics models[17,18] nor geometric considerations as when the pore diameter increases by 50−90%, there is still just one ion in each pore contributing to charge storage and the remaining surface area and pore volume remain unused, decreasing the capacitance normalized by the pore surface or volume.

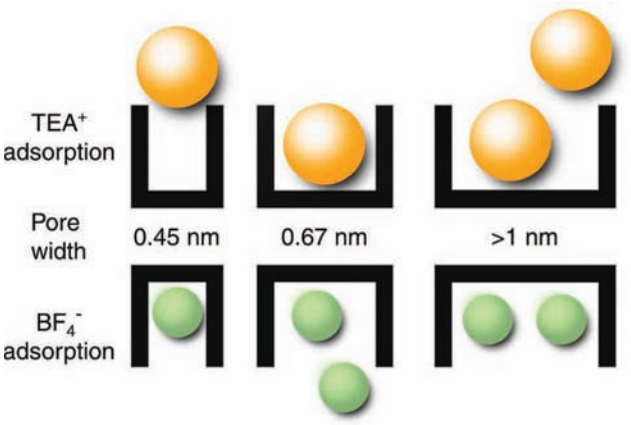

Figure 1. Electrosorption of specific ions with a finite size is only possible if the pore size is at least equal to the ion size. Therefore, the specific surface area of pores smaller than the bare ion size is inaccessible for energy storage. Larger pores can adsorb more than one ion per pore.

Recently, we developed a model for understanding the capacitance of microporous carbons, taking into account the entire measured pore size distribution, and have established a comprehensive data set of electrochemical measurements.[6] Density functional theory (DFT) kernels were used, which are currently the most advanced methodology to extract porosity data from gas sorption isotherms for meso- and microporous carbons and effectively avoid the fundamental limitations of the BET theory.[19] Activated carbon showed the highest specific surface area (SSA), followed by two different titanium carbide-derived carbons (CDCs),[20] activated carbon black (CB), and carbon onions.[21] Yet, when normalizing electrochemical performance data on porosity values, we first have to consider differences between dry powder and film electrodes.[6] Then, we have to assess the differences in pore size distributions; these are shown in Figure 2A normalized to 100% for the aforementioned carbon materials. Many carbons display a significant dispersion width; this is why the often-used volume-weighted average pore size d_{50} does not fully capture the pore size distribution width, as we show by adding values for d_{25} and d_{75}, representing the pore width encompassing 25 and 75% of the total pore volume, respectively (Table 1, Figure 2A).

More differences in the surface area of the different electrode materials become evident when we calculate the electrochemically active surface, that is, the ion-accessible surface area (Table 1, Figure 2B). Taking into account the bare ion size of BF_4^- (0.45 nm) and TEA^+ (0.67 nm), pores smaller than these

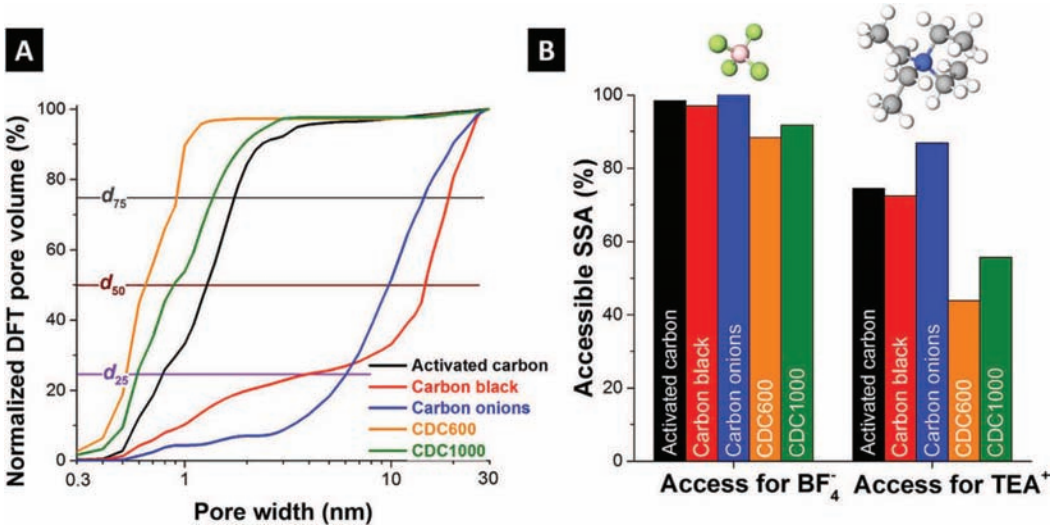

Figure 2. (A) The cumulative pore size distribution of electrodes was derived by combining CO_2 and N_2 sorption and normalizing all data to 100%. (B) Porosity analysis of different carbon electrode materials using a DFT model. Data are normalized for SSA of electrodes containing 10 mass% PTFE as 100% and the calculated accessible surface area for BF_4^- anions (0.4 nm, BF_4^- accessible) and TEA^+ cations (0.6 nm, TEA^+ accessible).

Table 1. Combined NLDFT Model for CO_2 Sorption for Pores Smaller than 0.9 nm and QSDFT Model for N_2 Sorption for Pores Larger than 0.9 nm[a]

Material	DFT SSA ($m^2 \cdot g^{-1}$)	$d_{50}(d_{25}–d_{75})$ pore width (nm)	capacitance at +1 V in ACN ($F \cdot g^{-1}$)	Coulomb efficiency (%)	capacitance at +1 V in PC ($F \cdot g^{-1}$)	Coulomb efficiency (%)	capacitance at −1 V in ACN ($F \cdot g^{-1}$)	Coulomb efficiency (%)	capacitance at −1 V in PC ($F \cdot g^{-1}$)	Coulomb efficiency (%)
AC	1839	1.3 (0.8–1.8)	113	96	115	99	103	99	102	99
CB	1097	15 (5–19)	99	99	99	99	88	99	87	99
OLC	232	9.5 (6–14)	20	98	20	99	16	99	16	99
CDC600	934	0.64 (0.53–0.93)	127	97	132	98	121	98	119	99
CDC1000	967	0.90 (0.62–1.4)	101	97	100	98	98	98	96	99

[a]The average pore size relates to the volume-weighted arithmetic mean value d_{50} with the standard deviation from d_{25} to d_{75}. Capacitance values were recorded at +1 V vs carbon and −1 V vs carbon in a three-electrode setup (half-cell).

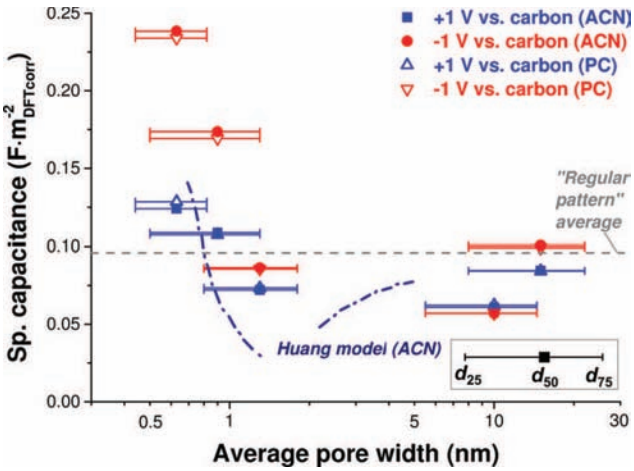

Figure 3. Capacitance of porous carbons normalized to the accessible surface area for each ion in both solvents. The regular pattern average of 0.95 F m^{-2} from ref 15 is added, and data for the Huang model is from ref 17.

values are inaccessible to the ions.[7] The result is a further reduction of the specific surface area, and we have to consider different cutoff values for the positively (cutoff pore size of 0.4 nm) and negatively (cutoff at 0.6 nm) polarized electrodes. In the case of CDC, only about 40–50% of the total SSA is accessible to TEA^+ compared to about 70% for activated carbon and carbon black (Figure 2A).

The reported electrochemical measurements using a three-electrode configuration (for experimental methods see the Supporting Information) showed a nonlinear correlation of SSA and gravimetric capacitance measured in $F \cdot g^{-1}$ (Table 1) for 1 M TEA-BF_4 in acetonitrile (ACN) or propylene carbonate (PC).[6] A very high Coulombic efficiency (up to 99%) underlines the absence of significant Faradaic reactions in the chosen potential window (Table 1). When we normalize the measured electrode capacitance by the surface area accessible to cations or anions at +1 and −1 V vs carbon, respectively, we see a clear difference between positive and negative polarization (Figure 3, Table 1). Instead of just discussing the electrochemical data in the context of average pore width (d_{50}), we added error bars for the x-axis, which spread between d_{25} and d_{75} (Figure 3). Even when considering pore size dispersity, we still see a clear trend of increased normalized capacitance in subnanometer pores, which is significantly larger for negative polarization (i.e., electrosorption of the larger TEA^+ cation). The more effective use of available pores in the case of matching sizes results in a strong increase in capacitance, which was already shown by a geometric model of Huang et al. (ref 22; see also the data line in Figure 3). For larger pore sizes, in

particular, for mesopores, the capacitance converges toward an average value below 0.1 $F \cdot m^{-2}$, which aligns well with the "regular pattern" value reported by Centeno et al. (ref 15) and with the calculated value limiting the double-layer capacitance at the planar carbon interface (or larger than the few-nm pores; ref 17).

For electrolytes with significant differences between the size of anions and cations, our data clearly show the importance of differentiating between ion electrosorption during positive or negative polarization with use of half-cell measurements (Figure 3). With a larger size of TEA^+, and smaller corresponding surface area accessible to the cations, the values of areal capacitance during negative polarization are significantly larger than those for BF_4^- electrosorption (i.e., positive polarization). Accordingly, advanced EDLC cell design could achieve performance enhancement by developing nanoporous carbon with slightly different pore sizes for the positive and negative electrodes.[23,24]

In summary, our data analysis clearly supports the increase in surface-normalized capacitance when most of the pores are below 1 nm, in agreement with previous studies (e.g., see refs 7 and 25). This was shown for carbons with very different pore structures considering the complexity of pore size dispersity and for two different solvents (i.e., PC and ACN). This effect is seen at different amplitudes for positive and negative polarization, with a smaller increase for BF_4^- within the range of investigated pore sizes.

Nicolas Jäckel[†,‡]
Patrice Simon[*,§,∥]
Yury Gogotsi[*,⊥]
Volker Presser[*,†,‡]

[†]INM - Leibniz Institute for New Materials, 66123 Saarbrücken, Germany

[‡]Department of Materials Science and Engineering, Saarland University, 66123 Saarbrücken, Germany

[§]Université Paul Sabatier, CIRIMAT UMR, CNRS 5085, 5085, 31062 Toulouse Cedex 4, France

[∥]Réseau sur le Stockage Electrochimique de l'Energie, RS2E FR CNRS 3459, 80039 Amiens Cedex, France

[⊥]Department of Materials Science and Engineering, and A. J. Drexel Nanotechnology Institute, Drexel University, Philadelphia, Pennsylvania 19104, United States

AUTHOR INFORMATION

Corresponding Authors

*E-mail: simon@chimie.ups-tlse.fr (P.S.).
*E-mail: gogotsi@drexel.edu (Y.G.).
*E-mail: volker.presser@leibniz-inm.de (V.P.).

ACKNOWLEDGMENTS

The authors thank Dr. Weingarth, Dr. Aslan, Anna Schreiber, Jeon Jeongwook (all at INM), and Katherine Van Aken (Drexel University) for their technical support and helpful discussion. N.J. and V.P. also thank Prof. Eduard Arzt (INM) for his continuing support. Y.G. was supported by the Fluid Interface Reactions, Structures and Transport (FIRST) Center, an Energy Frontier Research Center funded by the U.S. Department of Energy, Office of Science, Office of Basic Energy Sciences.

REFERENCES

(1) Beguin, F.; Frackowiak, E. *Supercapacitors*; Wiley: Weinheim, Germany, 2013.
(2) Salanne, M.; Rotenberg, B.; Naoi, K.; Kaneko, K.; Taberna, P. L.; Grey, C. P.; Dunn, B.; Simon, P. Efficient storage mechanisms for building better supercapacitors. *Nature Energy* **2016**, *1*, 16070.
(3) Kondrat, S.; Perez, C. R.; Presser, V.; Gogotsi, Y.; Kornyshev, A. A. Effect of pore size and its dispersity on the energy storage in nanoporous supercapacitors. *Energy Environ. Sci.* **2012**, *5*, 6474−6479.
(4) Kastening, B.; Spinzig, S. Electrochemical polarization of activated carbon and graphite powder suspensions: Part II. Exchange of ions between electrolyte and pores. *J. Electroanal. Chem. Interfacial Electrochem.* **1986**, *214*, 295−302.
(5) Levi, M. D.; Sigalov, S.; Salitra, G.; Aurbach, D.; Maier, J. The effect of specific adsorption of cations and their size on the charge-compensation mechanism in carbon micropores: The role of anion desorption. *ChemPhysChem* **2011**, *12*, 854−862.
(6) Jäckel, N.; Rodner, M.; Schreiber, A.; Jeongwook, J.; Zeiger, M.; Aslan, M.; Weingarth, D.; Presser, V. Anomalous or regular capacitance? The influence of pore size dispersity on double-layer formation. *J. Power Sources* **2016**, *326*, 660−671.
(7) Chmiola, J.; Yushin, G.; Gogotsi, Y.; Portet, C.; Simon, P.; Taberna, P. L. Anomalous increase in carbon capacitance at pore sizes less than 1 nm. *Science* **2006**, *313*, 1760−1763.
(8) Raymundo-Pinero, E.; Kierzek, K.; Machnikowski, J.; Beguin, F. Relationship between the nanoporous texture of activated carbons and their capacitance properties in different electrolytes. *Carbon* **2006**, *44*, 2498−2507.
(9) Largeot, C.; Portet, C.; Chmiola, J.; Taberna, P.-L.; Gogotsi, Y.; Simon, P. Relation between the ion size and pore size for an electric double-layer capacitor. *J. Am. Chem. Soc.* **2008**, *130*, 2730−2731.
(10) Jiang, D.; Jin, Z.; Henderson, D.; Wu, J. Solvent effect on the pore-size dependence of an organic electrolyte supercapacitor. *J. Phys. Chem. Lett.* **2012**, *3*, 1727−1731.
(11) Feng, G.; Qiao, R.; Huang, J.; Sumpter, B. G.; Meunier, V. Ion distribution in electrified micropores and its role in the anomalous enhancement of capacitance. *ACS Nano* **2010**, *4*, 2382−2390.
(12) Segalini, J.; Iwama, E.; Taberna, P.-L.; Gogotsi, Y.; Simon, P. Steric effects in adsorption of ions from mixed electrolytes into microporous carbon. *Electrochem. Commun.* **2012**, *15*, 63−65.
(13) Levi, M. D.; Levy, N.; Sigalov, S.; Salitra, G.; Aurbach, D.; Maier, J. Electrochemical quartz crystal microbalance (EQCM) studies of ions and solvents insertion into highly porous activated carbons. *J. Am. Chem. Soc.* **2010**, *132*, 13220−13222.
(14) Thommes, M.; Kaneko, K.; Neimark, A. V.; Olivier, J. P.; Rodriguez-Reinoso, F.; Rouquerol, J.; Sing, K. S. W. Physisorption of gases, with special reference to the evaluation of surface area and pore size distribution. *Pure Appl. Chem.* **2015**, *87*, 1051−1069.
(15) Centeno, T. A.; Sereda, O.; Stoeckli, F. Capacitance in carbon pores of 0.7 to 15 nm: a regular pattern. *Phys. Chem. Chem. Phys.* **2011**, *13*, 12403−6.
(16) Garcia-Gomez, A.; Moreno-Fernandez, G.; Lobato, B.; Centeno, T. A. Constant capacitance in nanopores of carbon monoliths. *Phys. Chem. Chem. Phys.* **2015**, *17*, 15687−90.

(17) Huang, J.; Sumpter, B. G.; Meunier, V.; Yushin, G.; Portet, C.; Gogotsi, Y. Curvature effects in carbon nanomaterials: Exohedral versus endohedral supercapacitors. *J. Mater. Res.* **2010**, *25*, 1525−1531.
(18) Merlet, C.; Rotenberg, B.; Madden, P. A.; Taberna, P. L.; Simon, P.; Gogotsi, Y.; Salanne, M. On the molecular origin of supercapacitance in nanoporous carbon electrodes. *Nat. Mater.* **2012**, *11*, 306−10.
(19) Gor, G. Y.; Thommes, M.; Cychosz, K. A.; Neimark, A. V. Quenched solid density functional theory method for characterization of mesoporous carbons by nitrogen adsorption. *Carbon* **2012**, *50*, 1583−1590.
(20) Presser, V.; Heon, M.; Gogotsi, Y. Carbide-derived carbons − from porous networks to nanotubes and graphene. *Adv. Funct. Mater.* **2011**, *21*, 810−833.
(21) Zeiger, M.; Jäckel, N.; Aslan, M.; Weingarth, D.; Presser, V. Understanding structure and porosity of nanodiamond-derived carbon onions. *Carbon* **2015**, *84*, 584−598.
(22) Huang, J.; Sumpter, B. G.; Meunier, V. A universal model for nanoporous carbon supercapacitors applicable to diverse pore regimes, carbon materials, and electrolytes. *Chem. - Eur. J.* **2008**, *14*, 6614−6626.
(23) Sigalov, S.; Levi, M. D.; Salitra, G.; Aurbach, D.; Jänes, A.; Lust, E.; Halalay, I. C. Selective adsorption of multivalent ions into TiC-derived nanoporous carbon. *Carbon* **2012**, *50*, 3957−3960.
(24) Weingarth, D.; Zeiger, M.; Jäckel, N.; Aslan, M.; Feng, G.; Presser, V. Graphitization as a universal tool to tailor the potential-dependent capacitance of carbon supercapacitors. *Adv. Energy Mater.* **2014**, *4*, 1400316.
(25) Chmiola, J.; Largeot, C.; Taberna, P.-L.; Simon, P.; Gogotsi, Y. Desolvation of Ions in subnanometer pores and its effect on capacitance and double-layer theory. *Angew. Chem., Int. Ed.* **2008**, *47*, 3392−3395.

Supporting information

Increase in capacitance by subnanometer pores in carbon

N. Jäckel,[1,2] P. Simon,[3,4,*] Y. Gogotsi,[5,*] V. Presser[1,2,*]

[1] *INM - Leibniz Institute for New Materials, 66123 Saarbrücken, Germany*
[2] *Department of Materials Science and Engineering, Saarland University, 66123 Saarbrücken, Germany*
[3] *Université Paul Sabatier, CIRIMAT UMR, CNRS 5085, 5085, 31062 Toulouse Cedex 4, France*
[4] *Réseau sur le Stockage Electrochimique de l'Energie, RS2E FR CNRS 3459, France*
[5] *Department of Materials Science and Engineering & A. J. Drexel Nanotechnology Institute, PA 19104 Philadelphia, USA*

* Corresponding authors:
Patrice Simon: simon@chimie.ups-tlse.fr
Yury Gogotsi: gogotsi@drexel.edu
Volker Presser: volker.presser@leibniz-inm.de

Experimental Methods

A more detailed experimental description can be found in our earlier work (Ref. [1]). Activated carbon YP-50F from Kuraray (called AC) and carbon black BP2000 from Cabot (called CB) were used as received. Carbide-derived carbon (CDC) samples were derived from titanium carbide (TiC) by chlorine gas treatment at 600 °C (TiC600) or 1000 °C (TiC1000) for 3 h (in both cases). All samples were subsequently annealed at 600 °C in hydrogen for 2 h and after cooling placed in vacuum (0.1 mPa) for several hours to remove residual volatile gas species.[2] Carbon onions (OLC, stands for onion-like carbon) were derived from nanodiamond powder (NaBond) by thermal annealing in argon at 1700 °C for 1 h with a heating rate of 20 °C·min^{-1} (Thermal Technology Furnace).[3]

For electrode preparation, we added 10 mass% of polytetrafluoroethylene (PTFE, 60 mass% dispersion in water from Sigma Aldrich) as binder to the carbon powder, which was soaked with ethanol and ground in a mortar. The resulting dough-like material was further processed with a rolling machine (MTI HR01, MTI Corp.) to a 200±20 µm thick free standing film electrode and finally dried at 120 °C at 2 kPa for 24 h before use.

For electrochemical testing, we employed a custom-built polyether ether ketone (PEEK) cell with spring loaded titanium pistons as a three electrode system described elsewhere.[4] The working electrode was punched out with 12 mm diameter with a total mass of 10-20 mg. An overcapacitive YP-80F (Kuraray) electrode with 500 µm thickness and 25 mg served as counter electrode. We employed a glass-fiber separator (GF/A from Whatman) and a carbon-coated aluminum foil current collector (type Zflo 2653 from Coveris Advanced Coatings). PTFE-bound YP-50F was employed as a quasi-reference electrode with a potential close to 0 V vs. NHE.[5] The assembled cells were dried at 120 °C for 12 h at 2 kPa in an inert gas glove box (MBraun Labmaster 130, O_2 and H_2O <1 ppm) and, after cooling to room temperature, vacuum-filled with 1 M tetraethylammonium-tetrafluoroborate (TEA-BF_4) in electrochemical grade (i.e., water content <20 ppm) acetonitrile (ACN) or propylene carbonate (PC), both purchased from BASF. Electrochemical measurements were carried out using a VSP300 potentiostat/galvanostat from Bio-Logic, with galvanostatic cycling with potential limitation (GCPL) applying a 15 min holding step (e.g., at +1 V vs. carbon) to bring the system to an equilibrated state. The specific (gravimetric) capacitance during discharging was calculated via *Eq. (1)*:

$$C_{sp} = \frac{\int_{t_0}^{t_{end}} I dt}{U} \cdot \frac{1}{m}, \quad (1)$$

with specific capacitance C_{sp}, time t (t_0: starting time of discharge, t_{end}: end of discharging time), applied potential difference ΔE discharge current I, and total mass of the working electrode m (i.e., considering carbon and the binder). For every type of electrode composition, two electrodes were prepared and these two cells were tested individually to calculate mean values with a standard deviation always below 5 %.

Nitrogen gas sorption measurements were carried out with an Autosorb iQ system (Quantachrome) at the temperature of liquid nitrogen (-196 °C) after degassing at 150 °C for 10 h. For the measurements, the relative pressure (P/P_0) was varied from $5 \cdot 10^{-7}$ to 1.0 in 68 steps. The specific surface area (SSA) and pore size distribution (PSD) was calculated with the ASiQwin-software via quenched-solid DFT (QSDFT) kernel with a slit pore shape model between 0.56 and 37.5 nm.[6] As shown elsewhere, the error in assuming slit-like pores for OLC is not insignificant, but smaller than using other kernels.[4] Carbon dioxide gas sorption measurements were carried out at 0 °C in the relative pressure range from $1 \cdot 10^{-4}$ to $1 \cdot 10^{-2}$ in 40 steps. SSA and PSD values were calculated for pore sizes between 0.3 nm and 1 nm with the ASiQwin software using nonlocal density functional theory (NLDFT) kernel for CO_2 sorption.[7] 1D-NLDFT kernel suffer from the assumption of infinite flat, homogenous carbon surface which results in the incorrect pore size distribution with many sharp maxima and gaps in-between.[8] Nevertheless, CO_2 adsorption is the most favorable for measuring of ultramicropores.[9-10] The calculated PSD was incremented by a linear approximation of the calculated pore volume (CO_2-sorption-derived PSD was used up to a pore size of 0.9 nm and N_2-sorption-derived PSD for pores larger than 0.9 nm) to an equidistant point density as described elsewhere.[1]

References

1. Jäckel, N.; Rodner, M.; Schreiber, A.; Jeongwook, J.; Zeiger, M.; Aslan, M.; Weingarth, D.; Presser, V., Anomalous or regular capacitance? The influence of pore size dispersity on double-layer formation. *Journal of Power Sources* **2016,** *326* (1), 660-671.
2. Chmiola, J.; Yushin, G.; Gogotsi, Y.; Portet, C.; Simon, P.; Taberna, P. L., Anomalous increase in carbon capacitance at pore sizes less than 1 nanometer. *Science* **2006,** *313* (5794), 1760-1763.
3. Zeiger, M.; Jäckel, N.; Weingarth, D.; Presser, V., Vacuum or flowing argon: What is the best synthesis atmosphere for nanodiamond-derived carbon onions for supercapacitor electrodes? *Carbon* **2015,** *94* (1), 507–517.
4. Weingarth, D.; Zeiger, M.; Jäckel, N.; Aslan, M.; Feng, G.; Presser, V., Graphitization as a universal tool to tailor the potential-dependent capacitance of carbon supercapacitors. *Advanced Energy Materials* **2014,** *4* (13), 1400316.
5. Ruch, P. W.; Cericola, D.; Hahn, M.; Kötz, R.; Wokaun, A., On the use of activated carbon as a quasi-reference electrode in non-aqueous electrolyte solutions. *Journal of Electroanalytical Chemistry* **2009,** *636* (1-2), 128-131.
6. Gor, G. Y.; Thommes, M.; Cychosz, K. A.; Neimark, A. V., Quenched solid density functional theory method for characterization of mesoporous carbons by nitrogen adsorption. *Carbon* **2012,** *50* (4), 1583-1590.
7. Ravikovitch, P. I.; Vishnyakov, A.; Neimark, A. V., Density functional theories and molecular simulations of adsorption and phase transitions in nanopores. *Physical Review E* **2001,** *64* (1), 011602.
8. Jagiello, J.; Thommes, M., Comparison of DFT characterization methods based on N_2, Ar, CO_2, and H_2 adsorption applied to carbons with various pore size distributions. *Carbon* **2004,** *42* (7), 1227-1232.
9. Thommes, M.; Kaneko, K.; Neimark, A. V.; Olivier, J. P.; Rodriguez-Reinoso, F.; Rouquerol, J.; Sing, K. S. W., Physisorption of gases, with special reference to the evaluation of surface area and pore size distribution. *Pure Appl Chem* **2015,** *87* (9-10), 1051-1069.
10. Silvestre-Albero, J.; Silvestre-Albero, A.; Rodríguez-Reinoso, F.; Thommes, M., Physical characterization of activated carbons with narrow microporosity by nitrogen (77.4 K), carbon dioxide (273 K) and argon (87.3 K) adsorption in combination with immersion calorimetry. *Carbon* **2012,** *50* (9), 3128-3133.